

01 Mar 2009

## A Novel Long-Period Fiber Grating Optical Sensor for Large Strain Measurement

Genda Chen

*Missouri University of Science and Technology, gchen@mst.edu*

Hai Xiao

*Missouri University of Science and Technology, xiaoha@mst.edu*

Ying Huang

Zhi Zhou

*et. al. For a complete list of authors, see [https://scholarsmine.mst.edu/civarc\\_enveng\\_facwork/559](https://scholarsmine.mst.edu/civarc_enveng_facwork/559)*

Follow this and additional works at: [https://scholarsmine.mst.edu/civarc\\_enveng\\_facwork](https://scholarsmine.mst.edu/civarc_enveng_facwork)



Part of the [Civil Engineering Commons](#), and the [Electrical and Computer Engineering Commons](#)

---

### Recommended Citation

G. Chen et al., "A Novel Long-Period Fiber Grating Optical Sensor for Large Strain Measurement," *Proceedings of the Sensors and Smart Structures Technologies for Civil, Mechanical, and Aerospace Systems (2009, San Diego, CA)*, vol. 7292, no. PART 1, SPIE, Mar 2009.

The definitive version is available at <https://doi.org/10.1117/12.817715>

This Article - Conference proceedings is brought to you for free and open access by Scholars' Mine. It has been accepted for inclusion in Civil, Architectural and Environmental Engineering Faculty Research & Creative Works by an authorized administrator of Scholars' Mine. This work is protected by U. S. Copyright Law. Unauthorized use including reproduction for redistribution requires the permission of the copyright holder. For more information, please contact [scholarsmine@mst.edu](mailto:scholarsmine@mst.edu).

# A Novel Long-Period Fiber Grating Optical Sensor for Large Strain Measurement

Genda Chen<sup>1\*</sup>, Hai Xiao<sup>2</sup>, Ying Huang<sup>1</sup>, Zhi Zhou<sup>1,3</sup>, and Yinan Zhang<sup>2</sup>

<sup>1</sup>Department of Civil, Architectural, and Environmental Engineering, Missouri University of Science and Technology, Rolla, MO, 65401, U.S.A

<sup>2</sup>Department of Electric and Computer Engineering, Missouri University of Science and Technology, Rolla, MO, 65401, U.S.A

<sup>3</sup> School of Civil Engineering, Harbin Institute of Technology, Harbin 150090, P.R. of China

## Abstract

Critical buildings such as hospitals and police stations must remain functional immediately following a major earthquake event. Due to earthquake effects, they often experience large strains, leading to progressive collapses. Therefore, monitoring and assessing the large strain condition of critical buildings is of paramount importance to post-earthquake responses and evacuations in earthquake-prone regions. In this study, a novel large strain sensor based on the long period fiber grating (LPFG) technology is proposed and developed. CO<sub>2</sub> laser induced LPFG sensors are characterized for such mechanical properties as strain sensitivity in extension and flexure, sensor stability, and measurement range. For practical applications, the need for LPFG sensor packaging is identified and verified in laboratory implementations. By introducing various strain transfer mechanisms, the strain sensitivity of LPFG sensors can be customized for different applications at corresponding strain transfer ratios.

**Keywords:** Long Period Fiber Grating (LPFG), large strain, strain sensitivity, strain transfer, bending effect

## 1. Introduction

Under earthquake loads, building systems often experience large deformations, leading to the progressive collapse of their complete structures. Since critical buildings such as hospitals, power substations, fire and police stations are critical facilities to post-earthquake response and evacuation, they must remain functional immediately after an earthquake event. Therefore, monitoring and assessing the large strain condition of critical buildings is of paramount importance to earthquake-prone communities. Up to date, the most widely used tools for strain measurements are electrical resistance gauges, which were firstly proposed in 1856 by Lord Kelvin<sup>[1]</sup>. However, due to the electromechanical properties of the alloys, backing materials and the adhesives used in the resistance gauges, the maximum strain that can be measured prior to their failure is limited. Furthermore, wired strain gauges will likely lose their signals due to power outage during a strong earthquake when structures being monitored are subjected to large strains. For the same reason, conductive textiles that are operated with their electromechanical properties through a special design of “sensing string” will unlikely be functional during strong earthquakes even though they are capable of large strain measurements<sup>[2]</sup>. On the other hand, optical fiber sensors<sup>[3-5]</sup> that are corrosion resistant, high temperature tolerant and immune to electromagnetic interference are promising technologies for large strain measurement. In this category, the fiber Bragg grating (FBG) technology has been widely investigated and accepted in structural health monitoring communities. The other type of grating technology, namely long period fiber grating (LPFG), is much less studied. An FBG sensor couples two light strings in their respective forward- and backward-propagating core-guided modes near a resonant wavelength, functioning like a wavelength-selective mirror<sup>[6]</sup>. An LPFG sensor with a periodic refractive index perturbation of its fiber core has a period in the hundreds of micrometer and couples the guided light inside the fiber core into the cladding modes at certain discrete wavelengths (also known as resonance wavelengths)<sup>[7-9]</sup>. While a few large strain FBG sensors were presented<sup>[10]</sup>, large strain LPFG sensors have never been reported in the literature.

---

\* Corresponding author: gchen@mst.edu

Since its first inscription on optical fibers in 1996<sup>[7]</sup>, long period grating has been extensively investigated in sensing applications for temperature, strain, curvature, and ambient refractive index measurements<sup>[11-17]</sup>. However, the effects of various interrelated physical parameters on the sensitivity of LPFG sensors remain unclear in applications. To this endeavor, methods for the separation of different influence factors have been explored and presented<sup>[18-20]</sup>. Rego et al.<sup>[21]</sup> and Rao<sup>[22]</sup> presented a coupled temperature and strain sensor system based on arc-induced LPFGs and LPFG/MEFPI (micro extrinsic Fabry-Perot interferometric sensor). Bhatia et al.<sup>[23]</sup> demonstrated temperature-insensitive and strain-insensitive long-period gratings which were inscribed on conventional optical fibers. Wang<sup>[24]</sup> and Nam<sup>[25]</sup> reported some bending insensitive LPFG sensors which are induced either with a CO<sub>2</sub> laser and an electric arc. Other researchers<sup>[26]</sup> used the change of intensity for strain measurements with arc-induced LPFG sensors. To date, most of the research works about applications of LPFG sensing properties are focused on small strain condition. For large strain measurements, this study is aimed at developing a novel LPFG sensor packaged inside a steel tube. This study also characterizes the sensing properties of optical fibers that are inscribed with long period gratings induced by CO<sub>2</sub> lasers.

## 2. Measurement Principle of LPFG Sensing Systems for Large Strain

### 2.1 CO<sub>2</sub> laser induced LPFG sensor and measurement

A commonly-used optical fiber typically consists of a core and a cladding. It has a low residual stress at the core-cladding interface, which was induced during its manufacturing process. Long-period fiber grating (LPFG) is a process to periodically change the core-cladding difference in refractive index along the length of an optical fiber. Up to date, various ways have been reported for creating localized refractive index changes along an optical fiber, including UV light, electric arc discharge, focused infrared femtosecond laser pulses and CO<sub>2</sub> laser<sup>[25-29]</sup>. The grating method which has been used in this study is CO<sub>2</sub> laser irradiation. As shown in Fig. 1(a), for LPFGs inscribed in single-mode fiber (SMF), mode coupling happens when phase-matching condition between the fundamental core mode and a particular cladding mode is satisfied. The phase-matching condition required for coupling is given by<sup>[32]</sup>:

$$\lambda_{re}(n_{core} - n_{cladding}) = \Lambda \quad (1)$$

in which  $n_{core}$  and  $n_{cladding}$  are the effective indices of the guided core-mode and the cladding mode, respectively;  $\lambda_{re}$  is the center wavelength of the transmission resonance; and  $\Lambda$  is the period of refractive index modulation. The light traveling in cladding modes experiences a high loss, which gives attenuation bands at resonance wavelengths in the transmission spectrum. The transmission spectrum of a typical LPFG is shown in Fig. 1(b).

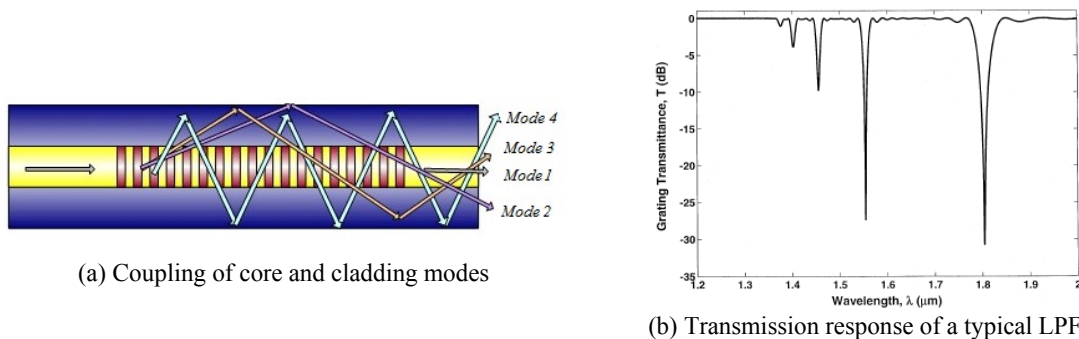
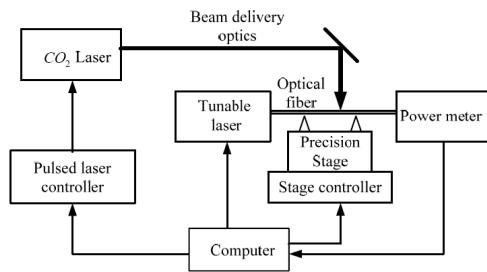


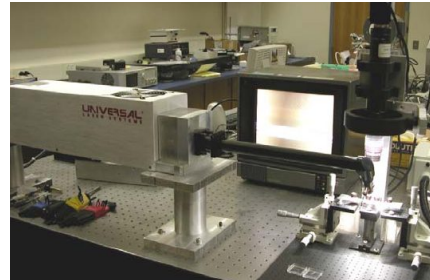
Fig. 1 Modes and transmission response of a typical LPFG

The schematic view and the prototype of the CO<sub>2</sub> laser based LPFG fabrication system are presented in Fig.2. A CO<sub>2</sub> laser (SYNRAD, Inc.) with a free space wavelength of 10.6μm and a maximum output power of 20W was used in the system. It is controlled by the computer through the laser controller to produce a desired power. The optical fiber (Corning SMF-28) with its buffer stripped is placed on a three dimensional (3D) motorized translation stage controlled by a computer, providing the option of displacing the translation stage in unison so that the fiber can be precisely moved to the center of the laser beam. The focused laser beam was transversely loaded onto the single mode optical fiber. Controlled by a computer, the translation stage moves the fiber at fixed step for laser exposure,

resulting in a periodic refractive index modulation in the fiber core. A microscope video camera was used to visualize the micro-displacement of the optical fiber while the fabrication process is activated. During grating fabrication, a tunable laser (HP81642A) and an optical power meter (HP 81618A) were also used to monitor the grating transmission spectrum<sup>[32]</sup>.



(a) Schematic of a CO<sub>2</sub> laser based LPFG fabrication system



(b) Photograph on the fabrication process

Fig. 2 Schematic view and prototype of the LPFG fabrication system and process

## 2.2 Strain transfer theories for large strain measurement

Bare optical fibers in tension can typically survive a strain of approximately 3,000  $\mu\epsilon$ . To measure large strains critical for engineering design, various strain transfer mechanisms have been investigated for embedded optical fiber sensors in recent years<sup>[33-35]</sup>. However, LPFG is sensitive to its surrounding environment so that it is not suitable to be embedded into any host structure without packaging and/or any protection. In this paper, two basic mechanisms are proposed as discussed below.

**Shear lag effect** Consider an LPFG optical fiber attached to a host material/structure and assume a rectangular section of the fiber with coating, as illustrated in Fig. 3<sup>[36]</sup>. Between the coated fiber ( $h_p$  thick) and the host material is an adhesive layer ( $h_a=h_0$  thick) that is used to transfer strain based on the shear lag effect from the host material to the optical fiber. A strain transfer ratio ( $STR < 1.0$ ) is defined as the strain ratio between the fiber and the host material.

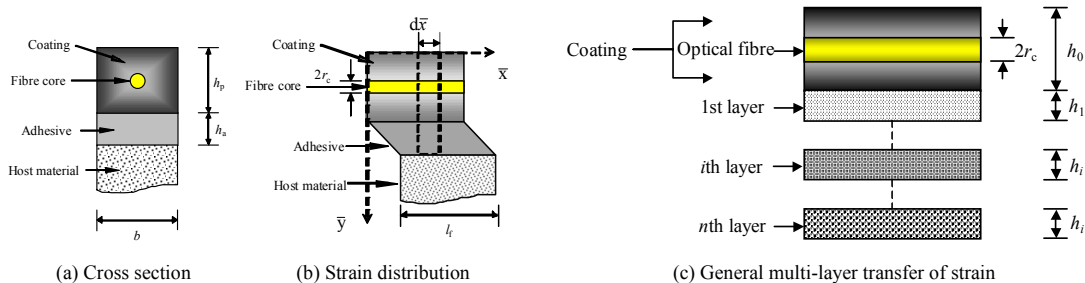


Fig.3 Strain transfer model with shear lag effect

For a general multi-layer system as shown in Fig. 3(c), the strain transfer ratio can be derived as<sup>[36]</sup>:

$$STR = \frac{\bar{\epsilon}_c}{\bar{\epsilon}_h} = 1 - \frac{\cosh(\lambda l_f) - 1}{\lambda l_f \sinh(\lambda l_f)} \quad \text{and} \quad \frac{1}{\lambda^2} = E_c h_0 \left[ \frac{(3h_0 - 2r_c)(h_0 + 2r_c)}{8h_0 G_0} + \sum_{i=1}^n \frac{h_i}{G_i} \right] \quad (2)$$

where  $\bar{\epsilon}_c$  and  $\bar{\epsilon}_h$  are the average strains of the optical fiber and the host material, respectively;  $l_f$  is the attachment length of the optical fiber;  $\lambda$  is an eigenvalue related to the adhesive layers as given in Equation (2) as well<sup>[36]</sup>;

$E_c$  and  $G_0$  are the Young's modulus and shear modulus of the optical fiber,  $G_i$  is the shear modulus of the  $i^{\text{th}}$  adhesive layer of  $h_i$  thick.

Since LPFG is highly sensitive to the environment and its transmission spectrum can be severely distorted by the adhesive coating, an LPFG sensor must be attached on its host structure at two points on two sides of the grating as indicated in Fig. 4 so that the grating is not in direct contact with the host structure. A specially designed adhesive layer can be introduced to transfer strain from the host structure to the LPFG sensor.

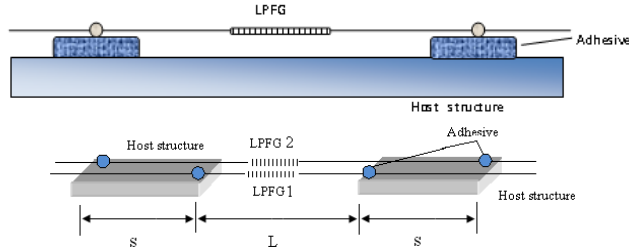


Fig. 4 Shear lag effect mechanism

Fig. 5 Gauge length change mechanism

**Gauge length change** From the mechanics of materials [37], it is well known that the average strain of a tension member is inversely proportional to the gauge length between two observation points. As such, by introducing a gauge length change mechanism, the strain in an LPFG attached on a structure can be significantly smaller than that of the structure, achieving a small STR value. As illustrated in Fig. 5, consider the two rigid blocks of a host structure move apart, resulting in deformation in LPFG1 and LPFG2 sensors. The LPFG1 measures the strain over a length,  $L$ , representing structural strain in practical applications, while the LPFG2 measures the strain over a length,  $L+2s$ . Therefore, the STR can be represented by

$$STR = \frac{\varepsilon_{LPFG2}}{\varepsilon_{structure}} = \frac{L}{L + 2s} \quad (3)$$

When  $s=L/2$ , Equation (3) gives rise to  $STR=0.5$ . For example, if the structure is subjected to  $3,000 \mu\varepsilon$ , the LPFG2 will measure  $1,500 \mu\varepsilon$  only, as a result of reduced deformation on the optical fiber.

### 3. Experiments and Test Results

#### 3.1 Calibration of LPFG sensors with tension tests

**Test setup and procedure** To relate the wavelength change of an LPFG sensor to the strain applied on the optical fiber, a series of tension tests were conducted with different cladding modes. As shown in Fig. 6, a weight was hung directly on an optical fiber inscribed with LPFG. Typical transmission spectra of an LPFG under various weights are presented in Fig. 7 in cladding mode 4. All tension tests were performed both in loading and unloading cycles to verify the repeatability of sensor readings.

**Results and discussion** The center wavelength of each transmission spectrum in Fig. 7 is determined and plotted in Fig.8 (a) as a function of the applied strain. Other test data and their linear regressions are presented in Fig.8 (b-d) for cladding mode 5-7. The sensitivities of the LPFG for different cladding modes are summarized in Table 1. It is observed from Fig. 8 that, at room temperature, the resonant wavelength of cladding modes 4 and 5 increases and that of cladding modes 6 and 7 decreases with the strain applied on the LPFG, resulting in a virtually “negative” sensitivity as listed in Table 1. This phenomenon is likely attributable to the fact that the resonant wavelength shift of a LPFG depends on both the grating period ( $\Lambda$ ) and the refractive index perturbation as indicated in Equation (1). Although the grating period always increases with the applied strain, the refractive index perturbation may vary with the applied strain differently depending upon the cladding modes of the grating. The combined effects of the parameters determine the positive or negative sensitivities as presented in Table 1.

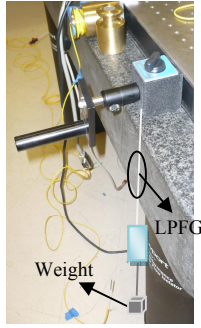


Fig. 6 Tension test setup

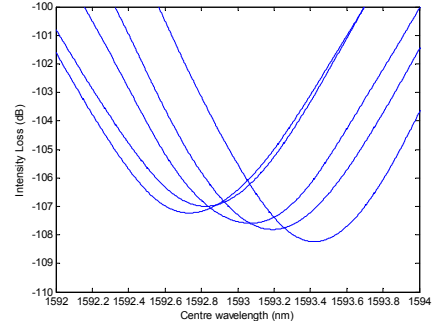
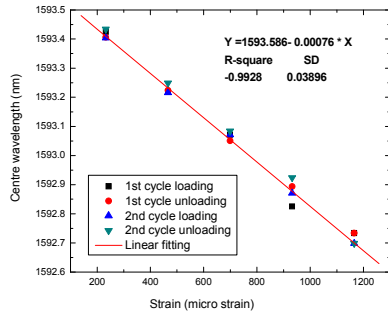
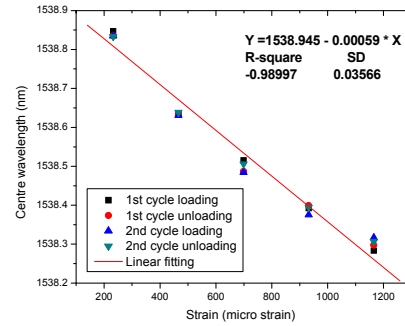


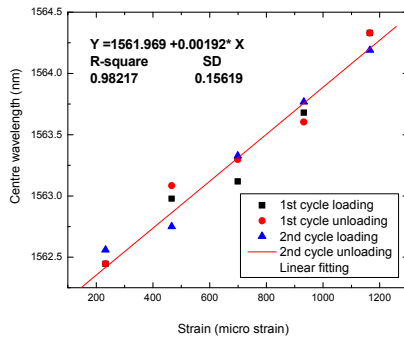
Fig. 7 Transmission spectra under various loads (cladding mode 4)



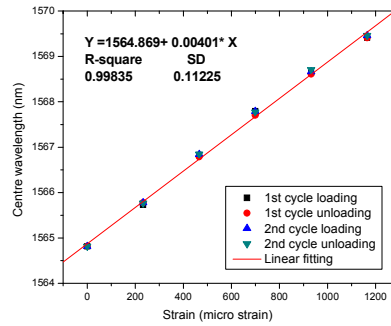
(a) Cladding mode 4



(b) Cladding mode 5



(c) Cladding mode 6



(d) Cladding mode 7

Fig. 8 Test data and linear fitting for LPFG sensor calibrations

Table1 Sensing properties of LPFG sensors

LPFG cladding mode	Initial center wavelength (nm)	Strain sensitivity (nm/ $\mu\epsilon$ )	Break strain ( $\mu\epsilon$ )
4	1593.586	-0.00076	2800
5	1538.945	-0.00059	3000
6	1561.969	+0.00192	3250
7	1564.869	+0.00401	3500

Fig. 8 also illustrates that the LPFG sensor has good linearity and repeatability for strain measurement. However, due to less released/weaker points as the mode of the LPFG sensor increases, its break strain increases correspondingly. Toward the goal of measuring large strains for the purpose of health monitoring of civil structures, LPFG sensors of higher cladding modes are more appropriate as they have better sensitivity and larger break strains.

### 3.2 Bending effect on LPFG measurements and necessity for LPFG packaging

**Test setup and procedure** LPFG sensors are brittle and sensitive to environmental factors such as moisture and temperature. Therefore, packaging of an LPFG sensor with a protective material such as glass tube is very desirable. An LPFG as a strain sensor attached on the tension side of a flexural member is subject to both bending and elongation. How the strain sensitivity of the LPFG sensor is affected by the combined bending and elongation effects remains unclear. To investigate the bending effect, a cantilevered tapered steel beam (with 1/8 inches thickness) was used. As shown in Fig. 9, under a concentrated load at the cantilever end, uniform strains are developed in the entire beam. Two sensors, LPFG1 and LPFG2, are installed on the tension side of the beam. LPFG1 is fixed at two attachment points with adhesives. LPFG2 is installed inside a glass tube of 150 $\mu$ m in diameter and anchored at both ends of the tube with adhesives. The glass tube is then supported by the steel beam with additional adhesives. The difference between the two sensors is that the LPFG2 is subjected to little bending effect since the glass tube is relatively stiffer than the adhesive attachments.

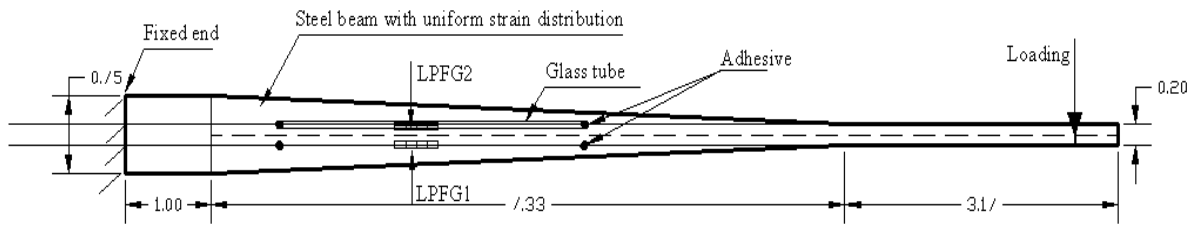


Fig. 9 Test setup of a cantilevered tapered steel beam (top view, all dimensions in inches)

**Test results and discussion** The relation between the center wavelength and the applied strain is presented in Fig.10 for LPFG1 and LPFG2 both with cladding mode 6. It can be seen from Fig.10 that the unpackaged LPFG1 loses its sensing properties due likely to strong bending effect. When packaged with the glass tube, LPFG2 can measure the applied strains satisfactorily. The strain sensitivity of the sensor is +0.00121 nm/ $\mu\epsilon$ , lower than the calibration sensitivity of +0.00192 nm/ $\mu\epsilon$  for mode 6 from Table 1. The reduction in strain sensitivity is mainly attributed to reduced bending effect or shorter elongation.

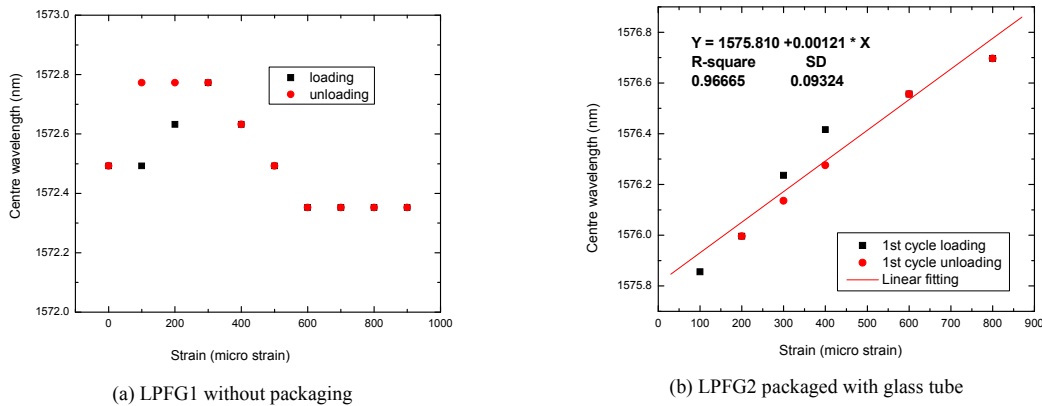


Fig.10 Bending effect on LPFG stability: cladding mode 6

The above observations indicate that an unpackaged LPFG sensor with cladding mode 6 is inappropriate for bending strain measurement. To ensure strain measurements, a bare LPFG with cladding mode higher than 6 or lower than 5 is a necessity. An alternative to solve this problem is to package an LPFG with a small glass tube. The glass tube can be as small as 150  $\mu$ m, which is slightly greater than the diameter of an optical fiber, 125  $\mu$ m.

### 3.3 Experimental verifications on strain transfer mechanisms

**Shear lag effect** A comparative experiment was designed with three attachment schemes of LPFG sensors as illustrated in Fig.11. LPFG1 is installed at the center points of two adhesive blocks; LPFG2 and LPFG3 are attached to two inner and outer points of the adhesive blocks, respectively. As shown in Fig. 12, the host structure is a tapered steel beam (with  $\frac{3}{4}$  inches thick, 12 inches long and 5 inches wide at the fixed end) that is cantilevered and subjected to uniform strain under a concentrated load at the tip of the tapered beam.

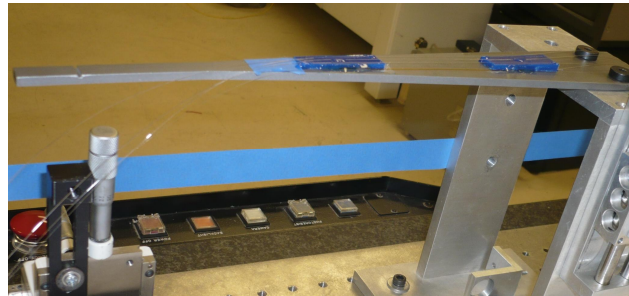
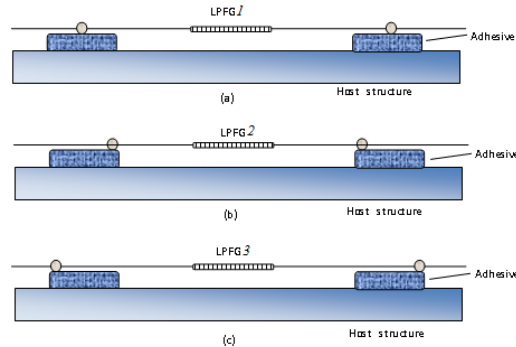
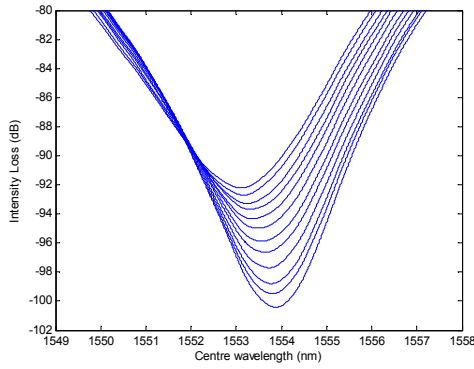


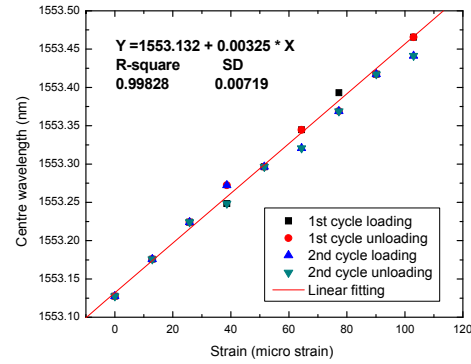
Fig. 11 LPFG attachment schemes

Fig. 12 Testing of cantilevered beam

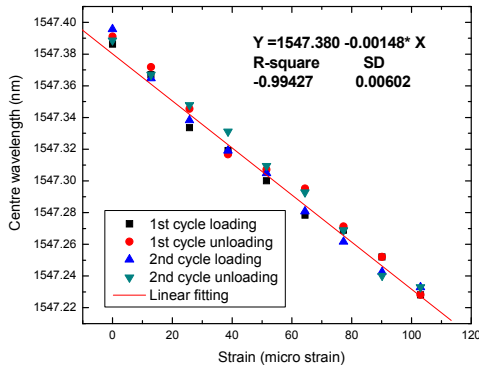
The transmission spectra at various loads for the case in Fig. 11(a) with cladding mode 7 are presented in Fig. 13(a). The center wave lengths at various loads are plotted as a function of the applied strains in Fig. 13(b). Similarly the relations between the center wavelength and the applied strain are shown in Fig.13(c, d) for the cases in Fig. 11(b, c) with cladding mode 5. It is clearly observed that the linear regression line for each case fits into the test data quite well. The strain sensitivities of all three cases shown in Fig.11 are summarized in Table 2. It can be observed from Table 2 that the strain sensitivity varies with the attachment points of the LPFG sensor. In comparison with the calibration sensitivity ( $+0.00401\text{nm}/\mu\epsilon$ ), the strain sensitivity ( $+0.00325\text{ nm}/\mu\epsilon$ ) remains high through multi-layer adhesives for the sensor attached at the center of adhesives. When attached at two inner points, the tension effect on the optical fiber is increased so that the strain sensitivity (negative value) increases nearly twice as much as of its corresponding calibration sensitivity. When attached at two outer points, the strain sensitivity (negative value) decreases more than twice its corresponding calibration sensitivity. In addition, the multi-layer adhesives not only change the strain sensitivity of the LPFG sensor but also reduce the bending effect on the LPFG. Although the LPFG with cladding mode 7 loses its strain sensitivity by approximately 20% due to bending effect, it generally works well under bending. For LPFG sensors with cladding mode lower than 6, the bending effect has increased the strain sensitivity to certain extent.



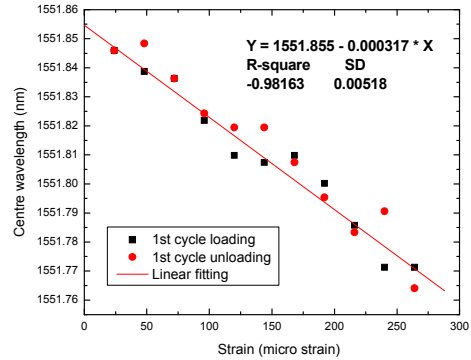
(a) LPFG1 transmission spectra (cladding mode 7)



(b) LPFG1 (cladding mode 7)



(c) LPFG2 (cladding mode 5)



(d) LPFG3 (cladding mode 5)

Fig.13 Demonstration of shear lag effect for strain transfer

Table 2 Sensing properties of LPFG sensors with multi-layer adhesives for strain transfer

Sensor designation	Support location	LPFG cladding mode	Initial center wavelength (nm)	Strain sensitivity (nm/ $\mu\epsilon$ )	Calibration sensitivity (nm/ $\mu\epsilon$ )
LPFG1	Center	7	1553.132	+0.00325	+0.00401
LPFG2	Inner	5	1547.380	-0.00032	-0.00059
LPFG3	Outer	5	1551.855	-0.00148	-0.00059

For large strain LPFG sensors, multi-layer adhesives with a certain length can be a promising mechanism for civil engineering applications. Engineers can use Equation (2) to choose adhesive material, layer thickness, and anchorage length in order to achieve various strain sensitivities for their application requirements.

**Gauge length change** A simple test as shown in Fig. 5 was set up to study the feasibility of strain transfer by gauge length changes. In this case, two sensors (LPFG1 and LPFG2 in cladding mode 4) were subjected to axial deformation. The center wavelength is related to the applied strain as presented in Fig.14. The sensing properties of the two sensors are summarized in Table 3. It is clearly seen from Table 3 that the strain sensitivity of the LPFG2 reduces more than half of its corresponding calibration value as the sensing gauge length increases by two times. This result verifies the strain transfer mechanism.

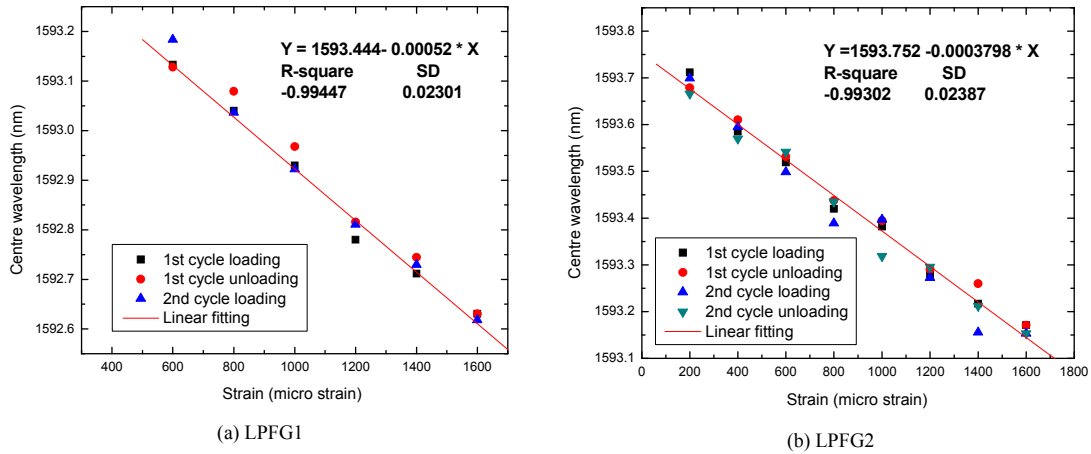


Fig.14 Demonstration of gauge length change effect: cladding mode 4

Table3 Sensing properties of LPFG sensors with gauge length changes for strain transfer

Sensor designation	LPFG Cladding mode	Initial center wavelength (nm)	Strain sensitivity (nm/με)	Calibration strain sensitivity (nm/με)
LPFG1	4	1593.444	-0.000521	-0.00053
LPFG2	4	1593.752	-0.000380	-0.00072

#### 4 Large Strain LPFG Sensors with a Hybrid Transfer Mechanism

The two basic strain transfer mechanisms discussed in the previous sections can be combined to develop a hybrid transfer mechanism as illustrated in Fig.15. This novel LPFG sensor has multi-layer adhesives at each end of the optical fiber that is placed inside a stiff structural member such as a steel tube that can be welded or a glass tube that can be attached with adhesive to the host structure at two points of L distance apart. The tube consists of two parts with a sleeve joint between the two supports on the host structure to facilitate their relative axial elongation. The strain measured with the LPFG sensor over the length (L+2s) is first converted to the strain between the two sensor attachment points of the tube, which is then converted to the average strain over the length (L). Therefore, the STR of the hybrid mechanism is actually equal to the multiplication of Equation (2) and Equation (3), shown as Equation (4). The steel or glass tube can protect the sensor from damage, environmental disturbance, and bending effect.

$$STR = \left( 1 - \frac{\cosh(\lambda(l-x)) - 1}{\lambda(l-x)\sinh(\lambda(l-x))} \right) \left( 1 - \frac{2y}{L+2y} \right) \quad (4)$$

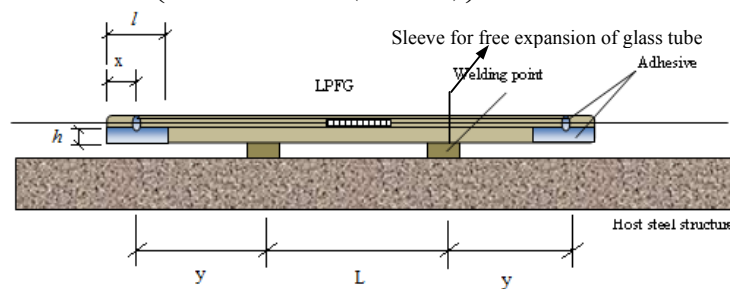


Fig.15 A novel LPFG sensor with hybrid strain transferring

A numerical example was designed to understand the performance of a hybrid strain transfer mechanism as shown in Fig. 15. It combines the two basic mechanisms used in Section 3, whose individual effectiveness has been demonstrated in Figs. 13 and 14. Fig. 16 compares the strain felt by LPFG with the strain in the host structure for four cases: without strain transfer effect, with shear lag effect, with gauge length change, and with shear lag & gauge length change (hybrid mechanism). In comparison with the benchmark without strain transfer, the slopes in Fig. 16 corresponding to the three mechanisms or STR values decreases in order with the use of shear lag, gauge length change, and hybrid mechanism. The calibration sensitivity without strain transfer is the highest. The effects of shear lag and gauge length change are similar in this example. The effect of the hybrid mechanism is approximately equal to the combined effects of both shear lag and gauge length change. As a result, the LPFG sensor with the hybrid mechanism can measure the level of strains in structures, 7,200  $\mu\epsilon$ . This level is approximately 2.5 times the break strain of the LPFG optical sensor.

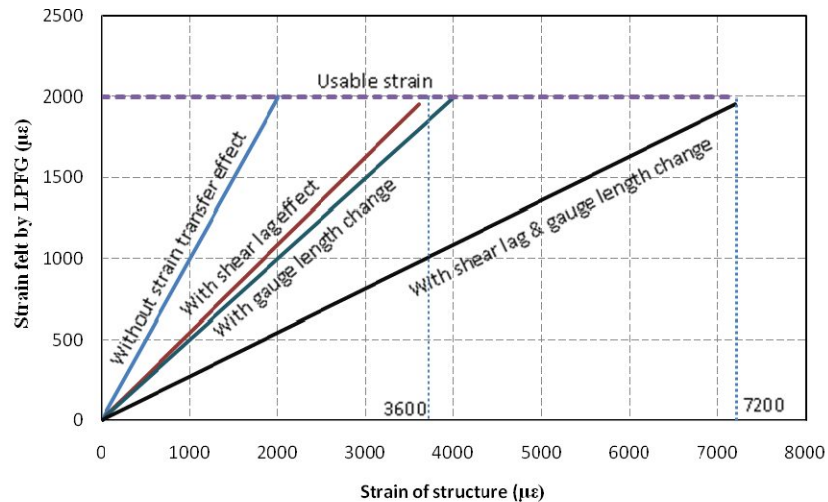


Fig. 16 Effects of various strain transfer mechanisms

## 5 Concluding Remarks

LPFG sensors with various cladding modes exhibit different tension strain properties. Both negative strain sensitivity with cladding mode 5 or lower and positive sensitivity with cladding mode 6 or higher were observed. However, detailed investigations are currently underway to understand their mechanisms. LPFG sensors are sensitive to temperature, strain, bending, environmental disturbance and damages. Thus, to ensure strain measurement under bending and protect LPFG from temperature, environmental disturbance and damage, packaging the LPFG sensor with a glass/steel tube is necessary. To make a bending insensitive sensor, LPFG with cladding mode lower than 5 or higher than 6 is recommended for practical applications. Experimental data demonstrated that LPFG sensors can only endure strain less than 3,500 $\mu\epsilon$  before their break. The break strain of the LPFG changes with its cladding mode. Higher break strains were observed for LPFGs with higher cladding modes. LPFG sensors of higher cladding modes are more appropriate as they have better sensitivity and larger break strains. In this paper, three strain transfer methods (shear lag, gauge length, and hybrid) were also studied and the sensing properties of each were characterized. The strain felt by a LPFG sensor can be adjusted by applying a multi-layer adhesives and/or changing sensing gauge length. The design optimization of the LPFG sensor for large strain measurement on civil structures will be studied in the near future.

## Acknowledgements

Financial support to complete this study was provided in part by the U.S. National Science Foundation under Award No. CMMI-0825942 with Dr. M.P. Singh as Program Director and by the Mid-America Transportation Center under

Award No. 0018358. The findings and opinions expressed in the paper are those of the authors only and do not necessarily reflect the views of the sponsors.

## References

1. Thomson W (Lord Kelvin) (1857). On the electro-dynamic qualities of metals. *Proc. R. Soc.* Vol. 8:546-50
2. Hui Zhang, Xiaoming Tao, Tongxi Yu, Shanyuan Wang and Xiaoyin Cheng (2006). A novel sensate 'string' for large-strain measurement at high temperature. *Meas. Sci. Technol.* Vol. 17:450-458
3. Sharon Kiesel, Kara Peters, Tasnim Hassan and Mervyn Kowalsky (2007). Behavior of intrinsic polymer optical fiber sensor for large-strain applications. *Meas. Sci. Technol.* Vol.18:3144-3154
4. KSC Kuang, ST Quekb, CY Tan, and SH Chew (2008). Plastic Optical Fiber Sensors for Measurement of Large Strain in Geotextile Materials. *Advanced Materials Research.* Vol. 47(50): 1233-1236
5. E. Udd, ed (1991). An Introduction for Scientists and Engineers. *Fiber Optic Sensors.* New York: John Wiley and Sons
6. A. Othonos and K. Kalli (1999). Fundamentals and Applications in Telecommunications and Sensing. *Fiber Bragg Gratings.* Boston: Artech House
7. A. M. Vengsarkar, J. R. Perdrazzani, J. B. Judkins, P. J. Lemaire, N. S., Bergano, and C. R. Davidson (1996). Long-period fibre gratings based gain equalizers. *Opt. Lett.* Vol. 21: 336-338
8. V. Bhatia and A. Vengsarkar (1996). Optical fibre long period grating sensors. *Opt. Lett.* Vol. 21:692-694
9. D. B. Stegall and T. Erdogan (2000). Dispersion control with use of long-period fiber gratings. *J. Opt. Soc. Am. A.* Vol. 17:304-312
10. Zhi Zhou, Chunguang Lan, and Jinping Ou (2006). New kind of FBG-based crack (large strain) sensor. *Proc. SPIE.* Vol. 6167:616714
11. H. J. Patrick, A. D. Kersey, and F. Bucholtz (1998). Analysis of the response of long period fibre gratings to external index of refraction. *J. Lightwave Technol.* Vol. 16: 1601-1611
12. H. J. Patrick, C. C. Chang, and S. T. Vohra (1998). Long period fibre gratings for structural bend sensing. *Electron. Lett.* Vol. 32 (18):1773-1775
13. W. J. Stephen and P. T. Ralph (2003). Optical fibre long period grating sensors: characteristics and application. *Meas. Sci. Technol.* Vol. 14:49-61
14. Nahar Singh, Subhash C. Jain, Vandana Mishra, G. C. Poddar, Ashu Kumar Bansal (2005). Mechanically created long-period fiber gratings as sensitive bend sensors. *Optical Engineering.* Vol. 44 (3):034403.1-034403.3
15. Patrick HJ, Chang CC, Vohra ST (1998). Long period fibre gratings for structural bend sensing. *Electron Lett.* Vol. 34 (18):1773-1775
16. Liu Y, Zhang L, Whllams JAR, Bennion I (2000). Optical bend sensor based on measurement of resonance mode splitting of long-period fiber grating. *IEEE Photonics Technol Lett.* Vol. 12:531-533
17. Chunn-Yenn Lin, Lon A. Wang and Gia-Wei Chern (2001). Corrugated Long-Period Fiber Gratings as Strain, Torsion, and Bending Sensors. *J. of Light wave Technology.* Vol. 19 (8):1159-1168
18. Yi-Ping Wang, Limin Xiao, D. N. Wang, and Wei Jin (2006). Highly sensitive long-period fiber-grating strain sensor with low temperature sensitivity. *Optics Letters.* Vol. 31 (23):3414-3416
19. Young-Geun Han and Sang Bae LEE (2005). Discrimination of Strain and Temperature Sensitivities Based on Temperature Dependence of Birefringence in Long-Period Fiber Gratings. *Japanese Journal of Applied Physics.* Vol. 44 (6A):3971-3974
20. Mei Nar Ng, Zhihao Chen, and Kin Seng Chiang (2002). Temperature Compensation of Long-Period Fiber Grating for Refractive-Index Sensing With Bending Effect. *IEEE Photonics Technology Letters.* Vol. 14 (3):361-362
21. G. Rego, J.R.A. Fernandes, J.L (2003). Santos and H.M. Salgado. New technique to mechanically induce long-period fibre gratings. *Optics Communications.* Vol. 220:111-118
22. Yun-Jiang Rao, Zeng-Ling Ran, Xian Liao, and Hong-You Deng (2007). Hybrid LPFG/MEFPI sensor for simultaneous measurement of high-temperature and strain. *Optics Express.* Vol. 15 (20): 14936-14947
23. Vikram Bhatia, David K. Campbell, Daniel Sherr, Tiffanie G. D'Alberto, Noel A. Zabaronic, Gregory A. Ten Eyck, Kent A. Murphy, Richard O. Claus (1997). Temperature-insensitive and strain-insensitive long-period grating sensors for smart structures. *Opt. Eng.* Vol. 36 (7):1872-1876

24. Y.P. Wang, Y.J. Rao, Z.L. Ran, T. Zhu, X.K. Zeng (2004). Bend-insensitive long-period fiber grating sensors. *Optics and Lasers in Engineering*. Vol. 41: 233-239
25. S. Nam, C. Zhan, J. Lee, C. Hahn, K. Reichard, P. Ruffin, K. -L. Deng, and S. Yin (2005). Bend-insensitive ultra short long-period gratings by the electric arc method and their applications to harsh environment sensing and communication. *Opt. Express*. Vol. 13:731-737
26. Alexey I. Kalachev, Vincent Pureur and David N. Nikogosyan (2005). Investigation of long-period fiber gratings induced by high-intensity femtosecond UV laser pulses. *Optics Communications*. Vol. 246:107-115
27. Y. Kondo, K. Nouchi, T. Mitsuyu, M. Watanabe, P. G. Kazansky, and K. Hirao (1999). Fabrication of long-period fiber gratings by focused irradiation of infrared femtosecond laser pulses. *Opt. Lett.* Vol. 24:646-648
28. D.D. Davis, T.K. Gaylord, E.N. Glytsis, S.G. Kosinski, S.C. Mettler and A.M. Vengsarkar (1998). Long-period fibre grating fabrication with focused CO<sub>2</sub> laser pulses. *Electron. Lett.* Vol. 34:302-303
29. L. Eldada (2004). Optical communication components. *Rev. Sci. Instr.* 75:575-593
30. B. H. Kim, Y. Park, T.-J. Ahn, D. Y. Kim, B. H. Lee, Y. Chung, U.C. Paek, and W.T. Han (2001). Residual stress relaxation in core of optical fibers by CO<sub>2</sub> laser irradiations. *Opt. Lett.* Vol. 26:1657-1659
31. Yanjun Li, Tao Wei, John A. Montoya, Sandeep V. Saini, Xinwei Lan, Xiling Tang, Junhang Dong and Hai Xiao (2008). Measurement of CO<sub>2</sub>-laser-irradiation-induced refractive index modulation in single-mode fiber toward long- period fiber grating design and fabrication. *Applied Optics*. Vol. 47 (29):5296-5304
32. Dusun Hwang, Linh Viet Nguyen, Dae Seung Moon and Young Joo Chung (2009). Intensity-based optical fiber strain sensor using long-period fiber gratings and a core mode blocker. *Meas. Sci. Technol.* Vol. 20: 034020.1-034020.6
33. Zhou Zhi, Li Jilong and Ou Jinping (2007). Interface transferring mechanism and error modification of embedded FBG strain sensors. *Frontiers of Electrical and Electronic Engineering in China*. Vol. 2 (1): 92-98
34. Zhou Guang-Dong, Li Hong-Nan, Liang ren, Li Dong-Sheng (2006). Influencing parameters analysis of strain transfer in optic fiber Bragg grating sensors. *Proceedings of SPIE*. Vol. 6179:61790.1-61790.9
35. C Y Wei, C C Ye, S W James, R P Tatam and P E Irving (2001). An experimental approach to qualify strain transfer efficiency of Fiber Bragg Grating sensors to host structures. *The 13th International Conference on Composite Materials, ICCM-13, Beijing*
36. Jilong Li, Zhi Zhou and Jinping Ou (2005). Interface strain transfer mechanism and error modification for adhered FBG strain sensor. *The International Society for Optical Engineering (SPIE-Int. Soc. Opt. Eng)*. Vol. 5851(1): 278-287
37. Robert D. Cook, Warren C. Young (1999). *Advanced mechanics of materials*. N.J.: Prentice Hall. 2nd edition.